Temperature-Independent Fermi Surface in the Kondo Lattice YbRh2Si2

K. Kummer, S. Patil, A. Chikina, M. Guettler, M. Hoeppner, A. Generalov, S. Danzenbaecher, S. Seiro, A. Hannaske, C. Krellner, et al.

Temperature-Independent Fermi Surface in the Kondo Lattice $YbRh_2Si_2$

K. Kummer,[1] S. Patil,[2] A. Chikina,[2] M. Güttler,[2] M. Höppner,[3,2] A. Generalov,[2] S. Danzenbächer,[2] S. Seiro,[4] A. Hannaske,[4] C. Krellner,[5] Yu. Kucherenko,[2,6] M. Shi,[7] M. Radovic,[7] E. Rienks,[8] G. Zwicknagl,[9] K. Matho,[10] J. W. Allen,[11] C. Laubschat,[2] C. Geibel,[4] and D. V. Vyalikh[2,12]

[1]*European Synchrotron Radiation Facility, 71, Avenue des Martyrs, Grenoble, France*
[2]*Institute of Solid State Physics, Dresden University of Technology, Zellescher Weg 16, D-01062 Dresden, Germany*
[3]*Max Planck Institute for Solid State Research, Heisenbergstrasse 1, D-70569 Stuttgart, Germany*
[4]*Max Planck Institute for Chemical Physics of Solids, Nöthnitzer Strasse 40, D-01187 Dresden, Germany*
[5]*Institute of Physics, Goethe University Frankfurt, Max-von-Laue-Strasse 1, D-60438 Frankfurt am Main, Germany*
[6]*Institute for Metal Physics, National Academy of Sciences of Ukraine, Vernadsky Boulevard 36, UA-03142 Kiev, Ukraine*
[7]*Swiss Light Source, Paul Scherrer Institut, Aarebrücke, CH-5232 Villigen, Switzerland*
[8]*Helmholtz-Zentrum Berlin, BESSY II, Albert-Einstein-Strasse 15, D-12489 Berlin, Germany*
[9]*Institut für Mathematische Physik, Technische Universität Braunschweig, Mendelssohnstrasse 3, D-38106 Braunschweig, Germany*
[10]*Institut Néel CNRS, and Université Joseph Fourier, 25 rue des Martyrs, BP 166, 38042 Grenoble cedex 9, France*
[11]*Randall Laboratory, University of Michigan, 450 Church Street, Ann Arbor, Michigan 48109, USA*
[12]*Department of Physics, St. Petersburg State University, St. Petersburg 198504, Russian Federation*

(Received 14 August 2014; revised manuscript received 19 December 2014; published 12 March 2015)

Strongly correlated electron systems are one of the central topics in contemporary solid-state physics. Prominent examples for such systems are Kondo lattices, i.e., intermetallic materials in which below a critical temperature, the Kondo temperature T_K, the magnetic moments become quenched and the effective masses of the conduction electrons approach the mass of a proton. In Ce- and Yb-based systems, this so-called heavy-fermion behavior is caused by interactions between the strongly localized $4f$ and itinerant electrons. A major and very controversially discussed issue in this context is how the localized electronic degree of freedom gets involved in the Fermi surface (FS) upon increasing the interaction between both kinds of electrons or upon changing the temperature. In this paper, we show that the FS of a prototypic Kondo lattice, $YbRh_2Si_2$, does not change its size or shape in a wide temperature range extending from well below to far above the single-ion Kondo temperature $T_K \sim 25$ K of this system. This experimental observation, obtained by means of angle-resolved photoemission spectroscopy, is in remarkable contrast to the widely believed evolution from a *large* FS, including the $4f$ degrees of freedom, to a *small* FS, without the $4f$'s, upon increasing temperature. Our results explicitly demonstrate a need to further advance in theoretical approaches based on the periodic Anderson model in order to elucidate the temperature dependence of Fermi surfaces in Kondo lattices.

DOI: 10.1103/PhysRevX.5.011028 Subject Areas: Strongly Correlated Materials

I. INTRODUCTION

Knowing the topology of the Fermi surface (FS) is a key ingredient for understanding the physical properties of crystalline solids [1,2]. The exotic low-temperature physics of strongly correlated electron systems, for instance, can often be directly ascribed to peculiarities in their FS. One example is the FS of itinerant antiferromagnets, i.e., spin-density-wave (SDW) systems [3]. In these materials, the FS contains congruent sheets that can be spanned by a single vector in $\boldsymbol{k}$ space and thus fulfills the necessary nesting conditions for the formation of a SDW [4]. In superconducting materials, the fundamental transition goes along with a gapping of the FS below the critical temperature T_c due to the formation of Cooper pairs. The symmetry of the superconducting gap can be obtained from the FS topology below T_c and different gap symmetries of s- [5], p- [6], and d-wave [7] type have been identified. Most of these observations have been made experimentally by means of angle-resolved photoemission spectroscopy (ARPES). Compared to the case of

superconductors, where interaction between two electrons gives rise to a gapped FS with depleted intensity at the Fermi energy (E_F) in ARPES, Kondo systems reveal a diametrically opposite behavior. In such systems, the interplay between localized spins and itinerant valence electrons generates a heavy-fermion state leading to a huge density of states close to the Fermi energy, the so-called Kondo resonance [8–10]. This resonance arises due to the formation of Kondo singlets where valence electrons screen local magnetic moments. This screening occurs below a characteristic temperature, which is called the single-ion Kondo temperature T_K.

In a regular lattice, the Kondo effect not only affects the magnitude of the density of states but also the momentum ($\boldsymbol{q}$) dependence of the quasiparticles, which manifests itself in a pronounced change of the FS. At low temperatures, the Fermi volume of a paramagnetic Kondo lattice is anticipated to include the f electron (f hole) in Ce (Yb) systems with one electron (hole) in the $4f$ shell due to Luttinger's theorem [11]. Upon weakening the interaction between $4f$ and valence electrons, the system is expected to undergo a transition to an ordered state of localized magnetic moments, and the $4f$ degree of freedom should be removed from the Fermi volume. While the change from the *large* to the *small* FS upon suppressing the f hybridization is nowadays evident from a large number of de Haas–van Alphen (dHvA) results on compounds that are either clearly intermediate valent or clearly stable trivalent [12], the way it occurs and the location where it occurs with respect to the transition from the paramagnetic to the magnetically ordered ground state is a matter of strong debate [13–16]. On the other hand, increasing temperature was also postulated to induce a change from the large to the small FS [17,18]. This was later supported by theoretical models [19]. Recent dynamical mean field theory (DMFT)-based numerical calculations gave an even more precise insight into this temperature-induced change of the FS, resulting in a broad acceptance of this idea [20,21]. However, despite a number of efforts, experimental evidence for the large-to-small FS transition with temperature is still weak and indirect [22–25].

II. RESULTS

The Kondo lattice material $YbRh_2Si_2$ is an ideal candidate to study how the FS reacts to the thermal damping of the heavy quasiparticles and to the onset of incoherent magnetic scattering [26]. It is known to be an excellent system for high-resolution ARPES studies, and the large FS seen at low temperatures has been studied in great detail [27–30]. The relevant temperature scale, $T_K \sim 25$ K, is known from specific heat C_p [26] and inelastic neutron scattering data [31] and is well accessible in ARPES experiments. The relevance of this scale in $YbRh_2Si_2$ is experimentally also confirmed by the temperature-dependent variations in the occupation of the $4f$ shell, which are characteristic of the Kondo effect.

A. Angle-integrated photoemission and resonant x-ray emission spectra

In photoemission, the onset of T dependence in the spectral weights can be seen already below 40 K for $YbRh_2Si_2$. Figure 1(a) shows a set of angle-integrated valence band photoemission spectra taken close to the $\bar{X}$-$\bar{\Gamma}$-$\bar{X}$ direction of the BZ at different temperatures between 1 and 40 K. Both the Yb $4f^{13}$ and the Yb $4f^{12}$ multiplet intensities of the $4f^{n-1}$ photoemission final state, corresponding to Yb^{2+} and Yb^{3+} ground-state configurations, respond to the rise in temperature, with the $4f^{13}$ intensity decreasing and the $4f^{12}$ intensity increasing. Figure 1(b) shows the Yb $L\alpha_1$ emission line for temperatures from 3 K to room temperature obtained by means of resonant x-ray emission spectroscopy (RXES) [32–34]. Clearly, the emission line is split into two well-defined subcomponents due to the different Coulomb interaction U_{vc} between valence electrons and the created $2p/3d$ core hole in the $4f^{14}$ (Yb^{2+}) and $4f^{13}$ (Yb^{3+}) configurations.

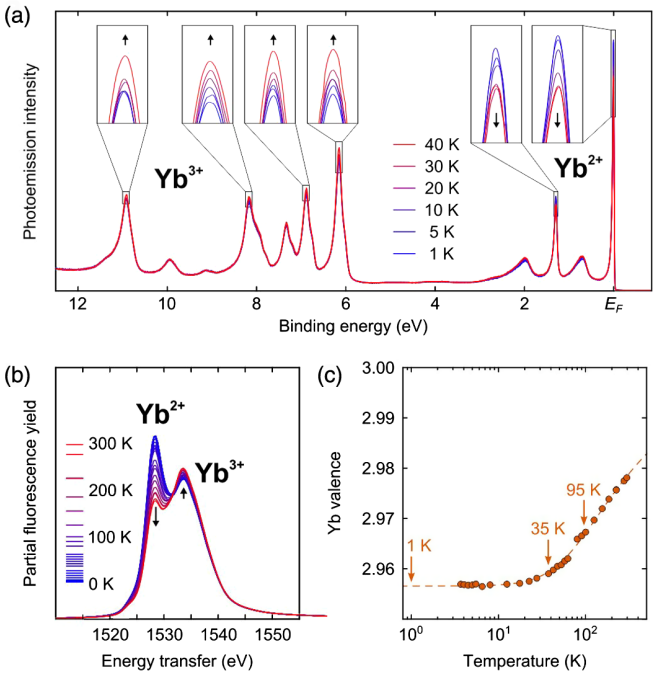

FIG. 1. Temperature dependence of the Yb valence in $YbRh_2Si_2$. (a) Angle-integrated photoemission intensity taken with high $4f$ sensitivity at 110 eV photon energy. There is a clear shift of weight from Yb^{2+} to Yb^{3+} with rising temperature, consistent with the single impurity Anderson model. (b) Yb $L\alpha_1$ RXES spectra from low to room temperature. A similar shift as in $4f$ photoemission from Yb^{2+} to Yb^{3+} is seen. The temperature-dependent Yb valence obtained from the $L\alpha_1$ spectra is shown on the right together with the best fit obtained within the noncrossing approximation to the Anderson impurity model.

The Yb valence can be determined from the intensities of the two subcomponents with very high accuracy [34]. This variation could also be fitted within a single impurity Anderson model approach [Fig. 1(c)]. A slow crossover towards unscreened Yb^{3+} ions sets in at about 20–30 K, which agrees well with the single-ion Kondo temperature $T_K \sim 25$ K of the material. The smallness of the variations and the overall closeness to $4f^{13}$ is a sign that charge fluctuations are almost frozen out, a prerequisite for the Kondo effect to occur [35].

B. Large and small Fermi surfaces

We are able to study the evolution of the FS between 1 and 95 K by means of ARPES, ensuring that a wide temperature range from far below to far above T_K is covered. In this range, notable changes should occur in the FS according to the heuristic picture that prevails in the scientific community. The low-temperature large FS of $YbRh_2Si_2$ far below T_K has already been well characterized by means of ARPES [27–30] and is shown in Fig. 2(b). The red starlike feature around the $\bar{M}$ point and the circlelike structure around the $\bar{\Gamma}$ point of the Brillouin zone stem from a Shockley-type surface state and a surface resonance, respectively, and thus reflect the surface electronic structure of the material. On the other hand, the orange squarelike feature, which is connected to its counterparts in the neighboring BZs by "necklike" features at the $\bar{X}$ point, derives from bulk bands. The holelike character of these

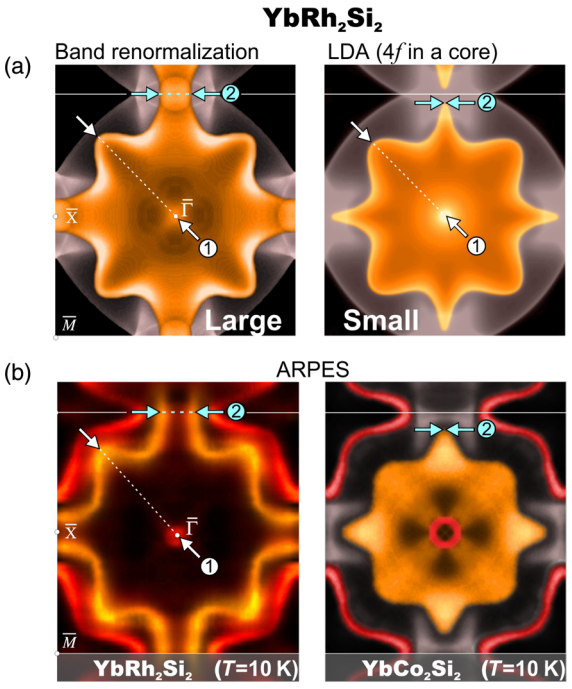

FIG. 2. (a) The large and small FS of $YbRh_2Si_2$ calculated within the renormalized band structure approach and the LDA scheme, respectively. (b) FS of $YbRh_2Si_2$ ($T_K = 25$ K) and $YbCo_2Si_2$ ($T_K < 1$ K) as seen in ARPES at $T \sim 10$ K.

bands around the Fermi energy is inherent to the FS of $YbRh_2Si_2$ and is clear evidence that a large FS is indeed seen at low temperatures.

We note that density functional theory based calculations indicate the presence of two large sheets in both the large and the small Fermi surfaces of $YbRh_2Si_2$, which have been named "donut" and "jungle gym" [36,37]. ARPES results reveal a clear signature only for the donut. Why the jungle gym is not seen is not completely understood, but a likely reason is that the ARPES signatures expected from the jungle gym are located in very close proximity to the pronounced surface state centered at the $\bar{M}$ point, and, therefore, are masked by the strong signal of this surface state.

The FS of $YbRh_2Si_2$ has also been investigated by dHvA experiments. The results do not match the predictions for the small or the large FS at zero magnetic field [36,37]. The reason for this discrepancy is now well understood: In $YbRh_2Si_2$, the large magnetic field used in the dHvA experiments ($B > 8$ T) induces strong changes in the Fermi surfaces, as clearly observed in transport measurements as a function of magnetic field [38,39]. These observations can be nicely explained by a renormalized band structure calculation including the effect of the magnetic field, which predicts a large change of the FS due to a strong polarization of the flat $4f$ bands and a weakening of the Kondo effect [38,40]. Notably, this gives a strong indication that the FS observed at large field in dHvA experiments emerges from a large FS at low field [40], in excellent agreement with our ARPES results.

The FS should shrink at higher temperatures where local moment screening breaks down and the screening electrons are transferred into the holelike bands, resulting in the small FS. The large and small FS calculated within the renormalized band structure approach [41] and the local-density approximations (LDA) scheme, respectively, are shown in Fig. 2(a). The two most obvious differences are in the region of the "necks" around the $\bar{X}$ point and in the overall size of the squarelike shape. The open necks of the large FS are due to a holelike d band with the apex just above E_F. They are closed in the small FS because the hole in the d band is filled and the band falls below E_F. Similarly, the size of the entire squarelike area is reduced for the small FS [Fig. 2(a)]. The calculated small FS of $YbRh_2Si_2$ agrees well with the experimental FS of the isoelectronic compound $YbCo_2Si_2$ at 10 K [Fig. 2(b)], which has an order of magnitude smaller T_K than $YbRh_2Si_2$ [42].

The transition from a large to a small FS would be best seen in energy cuts through the FS along the $\bar{M}$-$\bar{X}$-$\bar{M}$ and the $\bar{\Gamma}$-$\bar{M}$ directions, indicated by arrows labeled **1** and **2** in Fig. 2(a), respectively. The corresponding band maps are shown in Fig. 3 for an energy range of about 200 meV around E_F. Surprisingly, the FS does not change in the investigated temperature range within the sensitivity of our experiment, neither in the size of the squarelike part of the

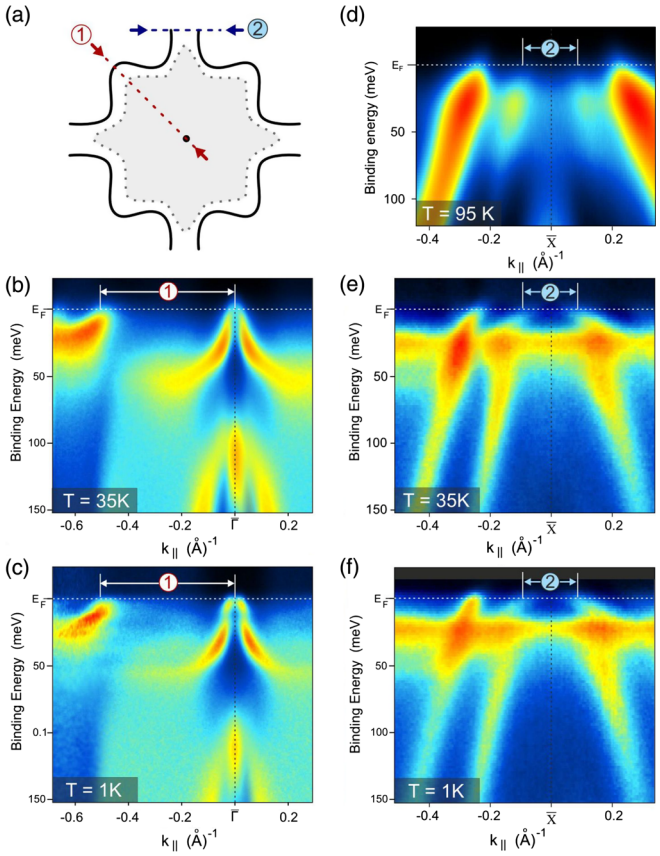

FIG. 3. Temperature-dependent FS evolution of $YbRh_2Si_2$. The T dependence is studied looking at two characteristic segments of the BZ that are schematically depicted in (a). (b),(c) "Diagonal" and (d)–(f) "neck" direction. The respective ARPES-derived energy-momentum maps are taken across the single-ion T_K and the "coherence" T^* temperatures. Note that the data shown in (d) are taken at another instrument with a different experimental geometry, leading to different sensitivities for $4f$ and valence states due to symmetry reasons. A detailed analysis of the spectral structure close to E_F at 95 K is presented in Fig. 4.

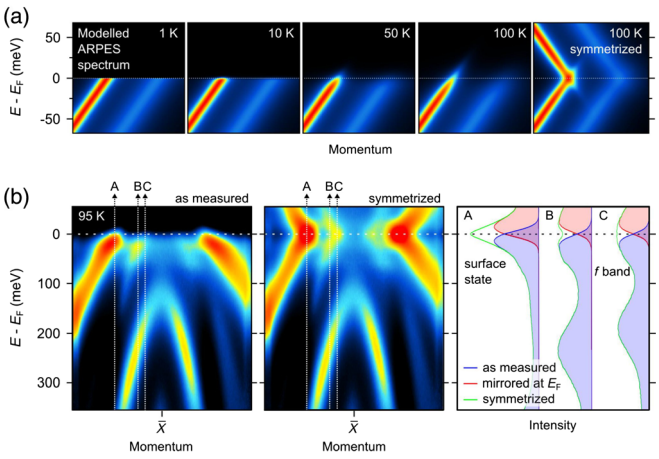

FIG. 4. (a) Thermal broadening due to the Fermi-Dirac statistics smears out the photoemission intensity symmetrically in an energy window $2k_BT$ around E_F, as it is shown for a model spectrum here. This makes it difficult to judge the presence or absence of spectral gaps at the Fermi level. A common way to analyze the spectral weight at E_F, which has been developed by the high-T_c community, is to symmetrize the ARPES spectra around E_F in order to overcome thermal broadening effects. (b) The 95 K ARPES data as measured [cf. Fig. 3(d)] and symmetrized around E_F. Following the intensity along the cuts A, B, and C, we see at E_F (A) enhanced spectral intensity as expected for the surface state, (B) a spectral gap where no band is crossing E_F, and (C) constant intensity at the position of the neck in Fig. 2 confirming that the f band is still crossing E_F and that the neck is still open at 95 K.

FS characterized by segment 1 nor in the opening of the necks characterized by segment 2. There are also no notable changes in the dispersion of the quasiparticle bands crossing E_F [28]. However, as we discuss latter, here we are limited by resolution and thermal broadening. Therefore, it is not straightforward to quantitatively address the temperature dependence of the quasiparticle width close to E_F. Qualitatively, however, within the temperature range studied, there are no signs in our data of jumps or sudden changes in the width occurring at some particular temperature. We consider this to be a strong indication that the quasiparticle width merely increases monotonically with increasing temperature.

To summarize our observations, the only notable change with temperature is the increased thermal broadening k_BT at 35 K and, especially, at 95 K compared to 1 K of otherwise unchanged ARPES spectra [28]. In particular, the characteristic neck of the large FS at the $\bar{X}$ point clearly remains open up to at least 95 K. Note that the already significant thermal broadening and the large intensity of the surface state in the 95 K data in Fig. 3(d) may give the impression of a spectral gap forming at E_F, which could be a sign of the neck closing. However, a detailed analysis of the spectral intensity at E_F, which is presented in Fig. 4, shows unambiguously that no such spectral gap is present at 95 K. Obviously, we do not observe the commonly expected transition from a large to a small FS as predicted, e.g., by a simplified slave-boson mean-field treatment [18]. The temperature-dependent valence change seen in angle-integrated PES and in RXES is not reflected in a simultaneous change of the FS.

III. DISCUSSION

The surprising absence of a change in the FS in our experimental results raises the question of whether we are studying the appropriate temperature range. While the change of the FS upon increasing T is a widely accepted idea now, the temperature range on which it takes place is less clear, because T-dependent properties of the Kondo lattice are still a challenge for theory. Experimentally, thermodynamic properties (specific heat C_p) and magnetic excitations (quasielastic width in inelastic neutron

scattering) in Kondo lattices are very similar to those in single-ion Kondo systems [8]. Therefore, the related energy scale, the single-ion T_K, is highly relevant also in Kondo lattices and can be determined quite precisely, with $T_K \sim 25$ K in $YbRh_2Si_2$ [31]. On the other hand, a strong difference between single-ion and lattice systems is observed in the T dependence of the resistivity $\rho(T)$. Kondo lattices display a maximum in $\rho(T)$ in a temperature range of 20–200 K followed by a very pronounced decrease towards low temperatures, which is associated with the onset of coherent screening [8]. In this regime, electron waves scattered from individual Kondo ions interfere coherently to form a narrow band of heavy electrons. This is also the supposed regime where the changes in the FS take place. In the conventional picture of coherence between screened magnetic sites, the temperature T^*, at which this coherence emerges, naturally cannot be higher than T_K [17]. However, in microscopic theory, the situation is very far from being clear, with some models getting a coherence temperature far below T_K [43], while others dispute the existence of a further independent energy scale besides T_K [44].

Experimentally, the coherence temperature T^* is usually determined from the temperature $T_{\max}$ of the maximum in $\rho(T)$. However, crystal-field effects also influence this maximum and can shift it to higher T [45]. This is likely the case in $YbRh_2Si_2$, where $T_{\max} \simeq 100$ K [26]. Thus, in the conventional picture based on transport measurements, one expects the change in the FS of $YbRh_2Si_2$ to occur well below 100 K. Interestingly, an investigation of this compound with STM, which is a probe closely related to ARPES in the sense that both give information on the one electron Green's function, observed the appearance of a peak in the tunneling conductance below 30 K, which was proposed to be related to the coherent state and from which $T^* \simeq 30$ K was deduced [46]. A further assessment of the T range, where the change of the FS is expected to occur, can be gained from a comparison with $CeIrIn_5$, which has a T_K very close to that of $YbRh_2Si_2$. Recent DMFT calculations for $CeIrIn_5$ predict the pronounced change in the FS to take place continuously between 10 and 80 K [20]. This range is centered on $T_K = 28$ K deduced from inelastic neutron scattering on this compound [47]. Thus, based on present knowledge and beliefs of Kondo lattices, the FS of $YbRh_2Si_2$ is expected to present at least some changes between 10 and 80 K. Up to now, there was no experimental evidence for a temperature above 100 K related to the formation of the coherent Kondo state [48].

On the other hand, in the single impurity case, the Kondo resonance is known to diminish in height and broaden as T is raised, but it remains visible for $T > 10T_K$. This motivated us to try a different theoretical approach to the temperature dependence of the FS. We start from the renormalized band structure approach, which is used to calculate the large FS in Fig. 2(a) and has proven to be very successful in the description of the change of the FS of $YbRh_2Si_2$ as a function of magnetic field [38]. The breakdown of the Kondo effect and the onset of decoherence upon increasing T is accounted for by using a suitable parametrization for the T dependence of the fully renormalized local $4f$ propagator as suggested previously (see Ref. [49] and references therein). The T-dependent parameters, i.e., the weight and width of the Kondo resonance, are chosen so as to reproduce the variation with T of the f valence [see Fig. 1(c)] and the depth of the Kondo dip in STM data [46]. In this approach, results of which are presented in Fig. 5, we find that the low-temperature state is formed via a slow crossover as known from the single-impurity problem [50]. In the calculations, the neck remains open until at least 120 K, i.e., far above T_K.

However, in Fig. 5, the calculations reveal a pronounced change in the width of the spectral function with temperature, as expected, which, e.g., results in a change of the apparent slope at E_F. Although we cannot resolve this width change in ARPES spectra because of the resolution of about 4 meV at low T and the strong thermal broadening at higher temperature, nonetheless, it has a strong effect on thermodynamic and transport properties. Therefore, the ARPES results do not contradict the increase of the effective mass, e.g., as observed in specific heat below 20 K, because the resolution is not sufficient to address this effect. On the other hand, the energy resolution of the present ARPES data is much smaller than the size of the hybridization gap, and, therefore, the $\boldsymbol{k}$-dependent hybridization as well as the size of the FS can be addressed quite precisely.

Looking for possible origins for the apparent discrepancy between the observation of a large FS in ARPES

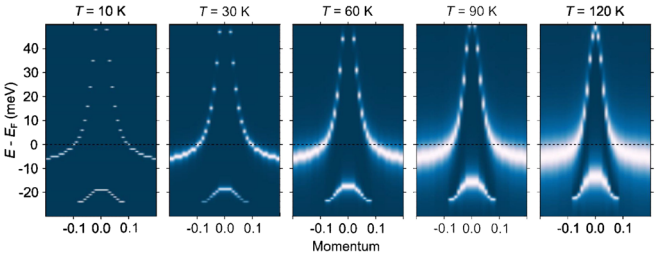

FIG. 5. $4f$ spectral functions corresponding to the crystal electrical field ground state calculated for temperatures $T = 10$, 30, 60, 90, and 120 K around the "neck" feature of the BZ. The calculations are performed within the renormalized band structure approach which has already been successful in calculating the large FS of $YbRh_2Si_2$ [Fig. 2(a)] and its change as a function of magnetic fields [40]. The calculated spectral function shows only a weak T dependence. The necks of the BZ remain open until well above 120 K, in accordance with the experimental result. To better visualize the changes in the distribution of $4f$ spectral weight, the spectra are normalized to the maximum value at the temperature under consideration.

up to 95 K and the disappearance of coherence in the T dependence of the resistivity at much lower temperatures, one should keep in mind that the coherence-related features in $\rho(T)$ appear in a temperature regime where the inelastic scattering of the magnetic degrees of freedom connected with the Kondo effect are already frozen out. The ARPES data, on the other hand, measure the $4f$ spectral function, which acquires momentum dependence due to hybridization with the dispersive conduction states. The present results unambiguously demonstrate that the $4f$ spectral function acquires the dispersion corresponding to the large FS before inelastic Kondo processes die out.

Our results have significant implications for the heavily debated question of where the transition from the large to the small FS occurs respective to the onset of magnetism upon weakening the f hybridization. Since this is currently a central issue in the field of Kondo lattices, we briefly review the current experimental knowledge. In Kondo lattice systems, antiferromagnetic (AFM) order is generally believed to emerge in a continuous, second-order-type transition at a quantum critical point (QCP), where quantum fluctuations result in very peculiar properties. In the so-called "local" or "Kondo breakdown" scenario, the change from the large FS to the small FS occurs exactly at the transition from the paramagnetic to the magnetic ordered ground state, i.e., at the QCP [13,14]. In contrast, in the so-called SDW scenario, the composite quasiparticles formed by hybridized $4f$ and valence states are maintained at the transition from the paramagnetic to the magnetic ordered ground state. Accordingly, the Fermi volume is supposed to change from the large one to the small one well within the magnetic ordered ground-state regime.

For a number of Ce-based Kondo lattices, dHvA experiments under pressure revealed an abrupt change in the spectra at the critical pressure separating the magnetic from the nonmagnetic ground state [51]. This was generally interpreted as a change from the small to the large FS. On the other hand, in a few Ce-based Kondo lattices, where the transition of magnetic to nonmagnetic was tuned by chemical substitution, the change of the FS did not seem to occur at the disappearance of the magnetic ordered ground state [52,53]. For Yb-based systems, similar experiments have not yet been reported. Nevertheless, the compound $YbRh_2Si_2$ has become one of the most disputed cases in this field, because pronounced anomalies in transport properties were taken as evidence for a Kondo breakdown at the field-induced suppression of the antiferromagnetic ground state [15,16]. Historically, the first observation of a pronounced change in the FS in a Kondo lattice upon tuning a parameter has been made at the metamagnetic transition in $CeRu_2Si_2$ [54,55]. While initially this change was interpreted as the switch from the large to the small FS, later on other mechanisms, like, e.g., a Zeeman-splitting-induced Lifshitz transition, were proposed [56,57]. Recently, it was demonstrated that the changes of the FS at higher magnetic fields in the Kondo lattice $YbRh_2Si_2$ involve a complex interaction between a smooth suppression of the Kondo effect and the spin splitting of the hybridized bands [38]. On the other hand, changes of the FS in high magnetic fields have also been reported for Ce compounds located in the magnetic ordered regime, but in this case, the changes seem to occur while keeping the Fermi volume small [58]. We note that within the Falicov-Kimball model [59], which played an important role in the very early days of valence fluctuating systems, a continuous change of the Fermi surface as a function of temperature or pressure was predicted [60].

Since $YbRh_2Si_2$ is located in the AFM ordered regime but extremely close to the QCP, one would expect to observe the small FS within the Kondo breakdown scenario, but the large FS within the SDW scenario [15]. Pronounced anomalies in the transport properties at the QCP connected with the suppression of the AFM in magnetic field were proposed to provide strong evidence for a Kondo breakdown scenario [61,62]. However, our observation of a large FS in ARPES in a large T range from 1 to 100 K is apparently a strong support for the SDW scenario and a strong challenge to the Kondo breakdown scenario. One might argue that the ARPES data are limited to temperatures above 1 K, and thus not relevant for the behavior at very low T, because there might be a change to the small surface upon cooling further down to the mK regime. However, the T-δ phase diagram (δ stands for the tuning parameter) proposed for the Kondo breakdown scenario indicates exactly the opposite behavior, see, e.g., Fig. 2(a) in Ref. [15]: with increasing T, the line E_{loc} separating the large from the small FS regime shifts to larger δ values, i.e., to larger hybridization strength. Hence, for a system like $YbRh_2Si_2$ with a magnetically ordered ground state, located on the left side of the critical point, the distance towards the large FS regime increases with temperature. In the Kondo breakdown scenario, one does not at all expect to observe a well-defined large FS at higher temperatures. In addition, we note that in $YbRh_2Si_2$, the Kondo breakdown was originally proposed to occur upon decreasing the magnetic field. The B-T phase diagram of $YbRh_2Si_2$ features a T^* line deduced from anomalies in many properties, and this line was proposed to correspond to the transition from the large FS at high fields to the small FS at low fields [62]. This line extends to temperatures well above $T_N = 70$ mK; in Ref. [15], e.g., it extends up to 3 K. Since there is compelling evidence that the FS at higher fields corresponds to the large one [38,40], our observation of a large FS in ARPES at zero field down to $T = 1$ K contradicts a transition from the large to the small FS upon decreasing field.

In summary, we explicitly demonstrate that the FS of the prototypical Kondo lattice $YbRh_2Si_2$ is remarkably stable in a wide temperature range around T_K. In particular, no signatures of the anticipated transition from localized to

itinerant $4f$ behavior are observed. The obtained experimental results seem to be strongly inconsistent with simplified mean-field treatments of the periodic Anderson model. At the same time, temperature-dependent variations of Yb^{2+} and Yb^{3+} features are evident in angle-integrated Yb $4f$ photoemission spectra and RXES spectra. How the variation of the local f valence is related to the coherent Kondo screening and what its effect on the FS topology is seems a more subtle problem. Our present study, in connection with recent STM results [46], suggests that the formation of the large FS occurs at a much higher temperature than the onset of coherence, i.e., both are not directly linked, in contrast to prevailing views. Further theoretical and experimental studies are needed in order to understand how the FS reacts on the crossover from coherence to incoherence in this particular Kondo lattice system and in Kondo lattices in general. Our observation of a large FS at 1 K supports a SDW scenario for the QCP in $YbRh_2Si_2$ and, thus, strongly questions the Kondo breakdown scenario. This scenario was proposed on the basis of the peculiar transport and thermodynamic properties observed in the vicinity of the QCP [13,14]. However, it was recently shown that these properties can be explained within a SDW scenario [16].

IV. METHODS

All ARPES experiments presented in this work have been performed at two synchrotron radiation facilities: BESSY II in Berlin (Germany) and Swiss Light Source (SLS) at the Paul Scherrer Institute in Villigen (Switzerland). At BESSY II, we used the One-Cubed ARPES instrument at the UE112-PGM1 beam line, while at SLS the experiments have been carried out at the SIS instrument. Both ARPES stations are equipped with a Scienta R4000 hemispherical electron analyzer. The SIS instrument offers a 6-axis CARVING manipulator with high angular precision, which is ideally suited to efficiently map Fermi surfaces and high-symmetry cuts along the Brillouin zone at temperatures down to 10 K. The BESSY II One-Cubed machine enables cooling down to ~1 K with ultrahigh-energy resolution at the cost of 2 degrees of freedom (azimuthal rotation of the sample and its tilt). The geometry of the experiments includes a fixed analyzer and a rotatable, vertically mounted sample. Note that the polar-angle rotation axis together with the direction of the analyzer slit was perpendicular (at BESSY II) and parallel (at SLS) to the plane of the storage ring. All samples are cleaved *in situ* in ultrahigh vacuum conditions at base pressures below 1×10^{-10} mbar. It is worth noting that both $YbRh_2Si_2$ and $YbCo_2Si_2$ samples are usually cleaved along the Si and Yb layers, where the interlayer bonding is relatively weak. By inspection of the ARPES signal as a function of the beam position on the sample, a surface region that is almost completely terminated by Si atoms is usually selected and then studied. To discriminate between valence band and $4f$ electron emissions, we use two photon energies: (i) at $h\nu = 45$ eV both kinds of states can be nicely seen in ARPES spectra while (ii) at $h\nu = 110$ eV, due to a Cooper minimum of the Rh $4d$ photoionization cross section, valence band emission is strongly reduced and emission from the $4f$ states dominates. Resonant X-ray emission experiments are performed at beam line ID16 of the ESRF in Grenoble (France). The accessible temperature range of the cryostat is 2.4–300 K. Calculations of the ARPES spectra are performed within the renormalized band structure approach which has already been successful in calculating the large FS of $YbRh_2Si_2$.

ACKNOWLEDGMENTS

This work was supported by the DFG (Grants No. VY64/1-3, No. GE602/2-3, and No. GRK1621).

[1] N. W. Ashcroft and N. David Mermin, *Solid State Physics* (Holt, Rinehart and Winston, New York, 1976).

[2] R. Ahuja, S. Auluck, P. Söderlind, O. Eriksson, J. M. Wills, and B. Johansson, *Fermi Surface of Noble Metals: Full-Potential Generalized-Gradient-Approximation Calculations*, Phys. Rev. B **50**, 11183 (1994).

[3] D. Li, J. Pearson, S. D. Bader, E. Vescovo, D.-J. Huang, P. D. Johnson, and B. Heinrich, *k-Space Origin of the Long-Period Oscillation in* Fe/Cr *Multilayers: A Photoemission Study of Epitaxial Cr Grown on an Fe(100) Whisker*, Phys. Rev. Lett. **78**, 1154 (1997).

[4] E. Fawcett, H. L. Alberts, V. Yu. Galkin, D. R. Noakes, and J. V. Yakhmi, *Spin-Density-Wave Antiferromagnetism in Chromium Alloys*, Rev. Mod. Phys. **66**, 25 (1994).

[5] H. Uchiyama, K. M. Shen, S. Lee, A. Damascelli, D. H. Lu, D. L. Feng, Z.-X. Shen, and S. Tajima, *Electronic Structure of* MgB_2 *from Angle-Resolved Photoemission Spectroscopy*, Phys. Rev. Lett. **88**, 157002 (2002).

[6] A. Damascelli, D. H. Lu, K. M. Shen, N. P. Armitage, F. Ronning, D. L. Feng, C. Kim, Z.-X. Shen, T. Kimura, Y. Tokura, Z. Q. Mao, and Y. Maeno, *Fermi Surface, Surface States, and Surface Reconstruction in* Sr_2RuO_4, Phys. Rev. Lett. **85**, 5194 (2000).

[7] A. Damascelli, Z. Hussain, and Z.-X. Shen, *Angle-Resolved Photoemission Studies of the Cuprate Superconductors*, Rev. Mod. Phys. **75**, 473 (2003).

[8] K. Andres, J. E. Graebner, and H. R. Ott, *4f-Virtual-Bound-State Formation in* $CeAl_3$ *at Low Temperatures*, Phys. Rev. Lett. **35**, 1779 (1975).

[9] A. A. Abrikosov, *Electron Scattering on Magnetic Impurities in Metals and Anomalous Resistivity Effects*, Physics **2**, 5 (1965).

[10] J. W. Allen, S.-J. Oh, M. B. Maple, and M. S. Torikachvili, *Large Fermi-Level Resonance in the Electron-Addition Spectrum of* $CeRu_2$ *and* $CeIr_2$, Phys. Rev. B **28**, 5347 (1983).

[11] R. M. Martin, *The Fermi Surface and Fermi Liquid Properties of Periodic Kondo and Mixed Valence Systems*, J. Appl. Phys. **53**, 2134 (1982).

[12] Y. Onuki and R. Settai, *de Haas–van Alphen Effect and Fermi Surface Properties in Rare Earth and Actinide Compounds*, Low Temp. Phys. **38**, 89 (2012).

[13] Q. Si, S. Rabello, K. Ingersent, and J. Lleweilun Smith, *Locally Critical Quantum Phase Transitions in Strongly Correlated Metals*, Nature (London) **413**, 804 (2001).

[14] P. Coleman, C. Pépin, Q. Si, and R. Ramazashvili, *How Do Fermi Liquids Get Heavy and Die?*, J. Phys. Condens. Matter **13**, R723 (2001).

[15] P. Gegenwart, Q. Si, and F. Steglich, *Quantum Criticality in Heavy-Fermion Metals*, Nat. Phys. **4**, 186 (2008).

[16] E. Abrahams and P. Wölfle, *Critical Quasiparticle Theory Applied to Heavy Fermion Metals near an Antiferromagnetic Quantum Phase Transition*, Proc. Natl. Acad. Sci. U.S.A. **109**, 3238 (2012).

[17] G. Zwicknagl, *Quasiparticles in Heavy Fermion Systems*, Phys. Scr. **T49A**, 34 (1993).

[18] P. Coleman, *Large N as a Classical Limit* $(1/N \approx \hbar)$ *of Mixed Valence*, J. Magn. Magn. Mater. **47–48**, 323 (1985).

[19] S. Burdin, A. Georges, and D. R. Grempel, *Coherence Scale of the Kondo Lattice*, Phys. Rev. Lett. **85**, 1048 (2000).

[20] H. C. Choi, B. I. Min, J. H. Shim, K. Haule, and G. Kotliar, *Temperature-Dependent Fermi Surface Evolution in Heavy Fermion* $CeIrIn_5$, Phys. Rev. Lett. **108**, 016402 (2012).

[21] A. Benlagra, T. Pruschke, and M. Vojta, *Finite-Temperature Spectra and Quasiparticle Interference in Kondo Lattices: From Light Electrons to Coherent Heavy Quasiparticles*, Phys. Rev. B **84**, 195141 (2011).

[22] D. Vasumathi, B. Barbiellini, A. A. Manuel, L. Hoffmann, T. Jarlborg, R. Modler, C. Geibel, F. Steglich, and M. Peter, *Fermi Surface of* $CeCu_2Si_2$ *by 2D Angular Correlation of Positron Annihilation Radiation*, Phys. Rev. B **55**, 11714 (1997).

[23] J. D. Denlinger, G.-H. Gweon, J. W. Allen, C. G. Olson, M. B. Maple, J. L. Sarrao, P. E. Armstrong, Z. Fisk, and H. Yamagami, *Comparative Study of the Electronic Structure of* XRu_2Si_2*: Probing the Anderson Lattice*, J. Electron Spectrosc. Relat. Phenom. **117–118**, 347 (2001).

[24] A. Koitzsch, S. V. Borisenko, D. Inosov, J. Geck, V. B. Zabolotnyy, H. Shiozawa, M. Knupfer, J. Fink, B. Büchner, E. D. Bauer, J. L. Sarrao, and R. Follath, *Hybridization Effects in* $CeCoIn_5$ *Observed by Angle-Resolved Photoemission*, Phys. Rev. B **77**, 155128 (2008).

[25] A. Koizumi, G. Motoyama, Y. Kubo, T. Tanaka, M. Itou, and Y. Sakurai, *f Electron Contribution to the Change of Electronic Structure in* $CeRu_2Si_2$ *with Temperature: A Compton Scattering Study*, Phys. Rev. Lett. **106**, 136401 (2011).

[26] O. Trovarelli, C. Geibel, S. Mederle, C. Langhammer, F. M. Grosche, P. Gegenwart, M. Lang, G. Sparn, and F. Steglich, $YbRh_2Si_2$*: Pronounced Non-Fermi-Liquid Effects above a Low-Lying Magnetic Phase Transition*, Phys. Rev. Lett. **85**, 626 (2000).

[27] S. Danzenbächer, D. V. Vyalikh, K. Kummer, C. Krellner, M. Holder, M. Höppner, Yu. Kucherenko, C. Geibel, M. Shi, L. Patthey, S. L. Molodtsov, and C. Laubschat, *Insight into the f-Derived Fermi Surface of the Heavy-Fermion Compound* $YbRh_2Si_2$, Phys. Rev. Lett. **107**, 267601 (2011).

[28] D. V. Vyalikh, S. Danzenbächer, Yu. Kucherenko, K. Kummer, C. Krellner, C. Geibel, M. G. Holder, T. K. Kim, C. Laubschat, M. Shi, L. Patthey, R. Follath, and S. L. Molodtsov, *k Dependence of the Crystal-Field Splittings of 4f States in Rare-Earth Systems*, Phys. Rev. Lett. **105**, 237601 (2010).

[29] D. V. Vyalikh, S. Danzenbächer, A. N. Yaresko, M. Holder, Yu. Kucherenko, C. Laubschat, C. Krellner, Z. Hossain, C. Geibel, M. Shi, L. Patthey, and S. L. Molodtsov, *Photoemission Insight into Heavy-Fermion Behavior in* $YbRh_2Si_2$, Phys. Rev. Lett. **100**, 056402 (2008).

[30] S. Danzenbächer, Yu. Kucherenko, D. V. Vyalikh, M. Holder, C. Laubschat, A. N. Yaresko, C. Krellner, Z. Hossain, C. Geibel, X. J. Zhou, W. L. Yang, N. Mannella, Z. Hussain, Z.-X. Shen, M. Shi, L. Patthey, and S. L. Molodtsov, *Momentum Dependence of 4f Hybridization in Heavy-Fermion Compounds: Angle-Resolved Photoemission Study of* $YbIr_2Si_2$ *and* $YbRh_2Si_2$, Phys. Rev. B **75**, 045109 (2007).

[31] O. Stockert, M. M. Koza, J. Ferstl, C. Geibel, and F. Steglich, *Low-Energy Spin Fluctuations in the Non-Fermi-Liquid Compound* $YbRh_2Si_2$, Sci. Tech. Adv. Mater. **8**, 371 (2007).

[32] C. Dallera, M. Grioni, A. Shukla, G. Vankó, J. L. Sarrao, J. P. Rueff, and D. L. Cox, *New Spectroscopy Solves an Old Puzzle: The Kondo Scale in Heavy Fermions*, Phys. Rev. Lett. **88**, 196403 (2002).

[33] L. Moreschini, C. Dallera, J. J. Joyce, J. L. Sarrao, E. D. Bauer, V. Fritsch, S. Bobev, E. Carpene, S. Huotari, G. Vankó, G. Monaco, P. Lacovig, G. Panaccione, A. Fondacaro, G. Paolicelli, P. Torelli, and M. Grioni, *Comparison of Bulk-Sensitive Spectroscopic Probes of Yb Valence in Kondo Systems*, Phys. Rev. B **75**, 035113 (2007).

[34] K. Kummer, Yu. Kucherenko, S. Danzenbächer, C. Krellner, C. Geibel, M. G. Holder, L. V. Bekenov, T. Muro, Y. Kato, T. Kinoshita, S. Huotari, L. Simonelli, S. L. Molodtsov, C. Laubschat, and D. V. Vyalikh, *Intermediate Valence in Yb Compounds Probed by 4f Photoemission and Resonant Inelastic X-Ray Scattering*, Phys. Rev. B **84**, 245114 (2011).

[35] Qualitatively, this behavior is in line with the photoemission result. It is, however, difficult to quantify the Yb valence changes from the photoemission data because of the surface sensitivity of the experiment and the ambiguities in the subtraction of the inelastic background [32].

[36] P. M. C. Rourke, A. McCollam, G. Lapertot, G. Knebel, J. Flouquet, and S. R. Julian, *Magnetic-Field Dependence of the* $YbRh_2Si_2$ *Fermi Surface*, Phys. Rev. Lett. **101**, 237205 (2008).

[37] A. B. Sutton, P. M. C. Rourke, V. Taufour, A. McCollam, G. Lapertot, G. Knebel, J. Flouquet, and S. R. Julian, *Observation of the J-Sheet of the Fermi Surface of* $YbRh_2Si_2$, Phys. Status Solidi (b) **247**, 549 (2010).

[38] H. Pfau, R. Daou, S. Lausberg, H. R. Naren, M. Brando, S. Friedemann, S. Wirth, T. Westerkamp, U. Stockert, P. Gegenwart, C. Krellner, C. Geibel, G. Zwicknagl, and F. Steglich, *Interplay between Kondo Suppression and Lifshitz Transitions in* $YbRh_2Si_2$ *at High Magnetic Fields*, Phys. Rev. Lett. **110**, 256403 (2013).

[39] A. Pourret, G. Knebel, T. D. Matsuda, G. Lapertot, and J. Flouquet, *Magnetic Polarization and Fermi Surface Instability: Case of* $YbRh_2Si_2$, J. Phys. Soc. Jpn. **82**, 053704 (2013).

[40] G. Zwicknagl, *Field-Induced Suppression of the Heavy-Fermion State in* $YbRh_2Si_2$, J. Phys. Condens. Matter **23**, 094215 (2011).

[41] S. Friedemann, S. Wirth, N. Oeschler, C. Krellner, C. Geibel, F. Steglich, S. MaQuilon, Z. Fisk, S. Paschen, and G. Zwicknagl, *Hall Effect Measurements and Electronic Structure Calculations on* $YbRh_2Si_2$ *and Its Reference Compounds* $LuRh_2Si_2$ *and* $YbIr_2Si_2$, Phys. Rev. B **82**, 035103 (2010).

[42] C. Klingner, C. Krellner, M. Brando, C. Geibel, F. Steglich, D. V. Vyalikh, K. Kummer, S. Danzenbächer, S. L. Molodtsov, C. Laubschat, T. Kinoshita, Y. Kato, and T. Muro, *Evolution of Magnetism in* $Yb(Rh_{1-x}Co_x)_2Si_2$, Phys. Rev. B **83**, 144405 (2011).

[43] S. Sykora and K. W. Becker, *Heavy Fermion Properties of the Kondo Lattice Model*, Sci. Rep. **3**, 2691 (2013).

[44] C. Grenzebach, F. B. Anders, G. Czycholl, and T. Pruschke, *Transport Properties of Heavy-Fermion Systems*, Phys. Rev. B **74**, 195119 (2006).

[45] Y. Lassailly, A. K. Bhattacharjee, and B. Coqblin, *Low-Temperature Resistivity and Magnetoresistivity of Cerium Compounds*, Phys. Rev. B **31**, 7424 (1985).

[46] S. Ernst, S. Kirchner, C. Krellner, C. Geibel, G. Zwicknagl, F. Steglich, and S. Wirth, *Emerging Local Kondo Screening and Spatial Coherence in the Heavy-Fermion Metal* $YbRh_2Si_2$, Nature (London) **474**, 362 (2011).

[47] T. Willers, Z. Hu, N. Hollmann, P. O. Körner, J. Gegner, T. Burnus, H. Fujiwara, A. Tanaka, D. Schmitz, H. H. Hsieh, H.-J. Lin, C. T. Chen, E. D. Bauer, J. L. Sarrao, E. Goremychkin, M. Koza, L. H. Tjeng, and A. Severing, *Crystal-Field and Kondo-Scale Investigations of* $CeMIn_5$ *(M = Co, Ir, and Rh): A Combined X-Ray Absorption and Inelastic Neutron Scattering Study*, Phys. Rev. B **81**, 195114 (2010).

[48] A few years ago, a phenomenological two-fluid model was proposed in which heavy-fermion systems are described in terms of two components, one representing the local moments while the second one, which appears only below the coherence temperature T^*, represents the hybridized heavy quasiparticles [63]. Within this model, a T^* value of 70 K has been proposed for $YbRh_2Si_2$ based on transport data. Our data clearly show that the *large* FS occurs for a temperature where this picture would predict it to be entirely *small*.

[49] K. Edwards, A. C. Hewson, and V. Pandis, *Perturbational Scaling Theory of the Induced Magnetization in the Impurity Anderson Model*, Phys. Rev. B **87**, 165128 (2013).

[50] The finding of $\log T$ dependencies for the dHvA frequencies and masses in Ref. [20] likely reflects the impurity Anderson model dynamics in DMFT and thus is very supportive of the view taken here.

[51] Y. Ōnuki, R. Settai, Y. Miura, H. Tsutsumi, F. Honda, and H. Harima, *Heavy-Fermion Superconductivity and Fermi-Surface Properties under Pressure*, Phys. Status Solidi B **250**, 583 (2013).

[52] Y. Matsumoto, M. Sugi, K. Aoki, Y. Shimizu, N. Kimura, T. Komatsubara, H. Aoki, M. Kimata, T. Terashima, and S. Uji, *Magnetic Phase Diagram and Fermi Surface Properties of* $CeRu_2(Si_{1-x}Ge_x)_2$, J. Phys. Soc. Jpn. **80**, 074715 (2011).

[53] C. Capan, Y.-J. Jo, L. Balicas, R. G. Goodrich, J. F. DiTusa, I. Vekhter, T. P. Murphy, A. D. Bianchi, L. D. Pham, J. Y. Cho, J. Y. Chan, D. P. Young, and Z. Fisk, *Fermi Surface Evolution through a Heavy-Fermion Superconductor-to-Antiferromagnet Transition: de Haas–van Alphen Effect in Cd-Substituted* $CeCoIn_5$, Phys. Rev. B **82**, 035112 (2010).

[54] H. Aoki, S. Uji, A. K. Albessard, and Y. Ōnuki, *Transition of f Electron Nature from Itinerant to Localized: Metamagnetic Transition in* $CeRu_2Si_2$ *Studied via the de Haas–van Alphen Effect*, Phys. Rev. Lett. **71**, 2110 (1993).

[55] F. S. Tautz, S. R. Julian, G. J. McMullan, and G. G. Lonzarich, *The Nature of Elementary Excitations below and above the Metamagnetic Transition in* $CeRu_2Si_2$, Physica (Amsterdam) **206–207B**, 29 (1995).

[56] R. Daou, C. Bergemann, and S. R. Julian, *Continuous Evolution of the Fermi Surface of* $CeRu_2Si_2$ *across the Metamagnetic Transition*, Phys. Rev. Lett. **96**, 026401 (2006).

[57] K. Miyake and H. Ikeda, *True Meaning of Localized f-Electrons Measured by dHvA Experiments in Ce-Based Heavy Fermion Metals*, J. Phys. Soc. Jpn. **75**, 033704 (2006).

[58] M. M. Altarawneh, N. Harrison, R. D. McDonald, F. F. Balakirev, C. H. Mielke, P. H. Tobash, J.-X. Zhu, J. D. Thompson, F. Ronning, and E. D. Bauer, *Fermi Surface of* $CePt_2In_7$*: A Two-Dimensional Analog of* $CeIn_3$, Phys. Rev. B **83**, 081103 (2011).

[59] R. Ramirez and L. M. Falicov, *Theory of the Alpha-Gamma Phase Transition in Metallic Cerium*, Phys. Rev. B **3**, 2425 (1971).

[60] V. V. Valkov and S. G. Ovchinnikov, *Some Peculiarities of de Haas–van Alphen Effect in Compounds with Intermediate Valence*, Sov. Phys. Solid State **23**, 2032 (1981).

[61] S. Paschen, T. Luhmann, S. Wirth, P. Gegenwart, O. Trovarelli, C. Geibel, F. Steglich, P. Coleman, and Q. Si, *Hall-Effect Evolution across a Heavy-Fermion Quantum Critical Point*, Nature (London) **432**, 881 (2004).

[62] P. Gegenwart, T. Westerkamp, C. Krellner, Y. Tokiwa, S. Paschen, C. Geibel, F. Steglich, E. Abrahams, and Q. Si, *Multiple Energy Scales at a Quantum Critical Point*, Science **315**, 969 (2007).

[63] Y.-f. Yang, Z. Fisk, H.-O. Lee, J. D. Thompson, and D. Pines, *Scaling the Kondo Lattice*, Nature (London) **454**, 611 (2008).